

Contents lists available at ScienceDirect

Petroleum Science

journal homepage: www.keaipublishing.com/en/journals/petroleum-science



Original Paper

Deciphering origins of hydrocarbon deposits by means of intramolecular carbon isotopes of propane adsorbed on sediments



Peng Liu ^{a, b}, Xiao-Feng Wang ^{b, *}, Jie Wang ^c, Juske Horita ^d, Zhi-Yong Wang ^c, Ying Lin ^e, Rui-Liang Guo ^f, Fu-Qi Li ^b, Wen-Hui Liu ^b

- ^a College of Safety Science and Engineering, Xi'an University of Science and Technology, Xi'an, 710054, Shaanxi, China
- ^b State Key Laboratory of Continental Dynamics, Department of Geology, Northwest University, Xi'an, 710069, Shaanxi, China
- ^c Exploration and Development Research Institute of PetroChina Tuha Oilfield Company, Hami, 839009, Xinjiang, China
- ^d Department of Geosciences, Texas Tech University, Lubbock, TX, 79409, USA
- ^e Department of Earth and Planetary Sciences, University of California, Riverside, CA, 92521, USA
- f School of Earth Sciences and Engineering, Xi'an Shiyou University, Xi'an, 710065, Shaanxi, China

ARTICLE INFO

Article history: Received 21 April 2024 Received in revised form 13 July 2024 Accepted 22 October 2024 Available online 24 October 2024

Edited by Jie Hao

Keywords: Hydrocarbon origins Intramolecular isotope distributions Position-specific isotope analysis (PSIA) Propane

ABSTRACT

Hydrocarbons are one of the important fluids within the Earth's crust, and different biotic and abitoic processes can generate hydrocarbon during geological periods. Tracing the sources and sinks of hydrocarbons can help us better understand the carbon cycle of the earth. In this study, an improved approach of adsorbed hydrocarbons extraction from sediments was established. The improved thermal desorption approach, compound-specific isotope analysis and position-specific isotope analysis were integrated to investigate the molecular and intramolecular isotope fractionation between trace hydrocarbon gases within sediments and geological hydrocarbon deposits. The isotopic compositions of the terminal position carbon of propane $(\delta^{13}C_{terminal})$ serves as a correlation indicator between trace hydrocarbon gases within sediments and geological hydrocarbon deposits. The tight sandstone gas from the Turpan-Hami Basin is a first case study for the application of this novel method to trace hydrocarbon origins. The results showed that the hydrocarbons in the tight sandstone gases in the study area most likely originated from humic organic matter (type III kerogen) at an early mature stage. $\delta^{13}C_{terminal}$ values of the thermally desorbed propane gases from different source rocks were distinguishable and the values of the tight sandstone gases significantly overlap with those of the Lower Jurassic Sangonghe source rocks, suggesting their genetic relationship. Overall, the results provided novel position-specific carbon isotopic constraints on origins of hydrocarbons.

© 2024 The Authors. Publishing services by Elsevier B.V. on behalf of KeAi Communications Co. Ltd. This is an open access article under the CC BY-NC-ND license (http://creativecommons.org/licenses/by-nc-nd/

1. Introduction

As one of the important fluids within the Earth's crust, hydrocarbons are characterized by diverse origins, including microbial processes, thermal cracking of organic matter, and inorganic chemical reactions (e.g. Fischer—Tropsch reaction) (Etiope and Schoell, 2014; Schoell, 1988; Smith and Pallasser, 1996; Vandré et al., 2007). These organic geofluids migrate within the crust from their sources to geological petroleum deposits and eventually to the atmosphere, playing a major role in the global carbon cycle

(Julien et al., 2020). For most hydrocarbons within the sedimentary basins, they are generally characterized by biogenic origins, such as microbial and thermogenic processes from organic matter within sediments (Claypool et al., 1980; Liu et al., 2019b; Schoell, 1983). Hydrocarbons are adsorbed onto the pores and surface of the minerals within the sources followed by generation and transported along the migration pathways in sediments. Therefore, trace gaseous hydrocarbons within source rocks (e.g. mudstone, shale, and coal) could represent in-situ hydrocarbons generated by organic matter, and their isotopic compositions may act as indicators to decipher hydrocarbon origins. However, isotopic fractionations between in-situ hydrocarbons within sources and accumulated hydrocarbon fluids are not well understood, hindering our ability to trace pathways from sources to sinks of

^{*} Corresponding author.

E-mail address: wangxf@nwu.edu.cn (X.-F. Wang).

hydrocarbon fluids during global carbon cycle.

In the past decades, compound-specific isotope analysis (CSIA) of gaseous hydrocarbons have been widely applied to tracing the origins of hydrocarbons (Dai et al., 2014; Liu et al., 2007, 2009, 2012, 2015, 2018b, 2018c; Schoell, 1980, 1988; Wang et al., 2015b; Xu, 1994). Relationships have been established between $\delta^{13}C_1$ of natural gases and the vitrinite reflectance ($\delta^{13}C_1$ - R_0 regression equations) for different types of sources (Chen et al., 2021; Galimov, 1988; Liu and Xu, 1999; Stahl and Carey, 1975; Xu, 1994). Those isotopic signatures and $\delta^{13}C_1$ - R_0 relationships are effective tools in tracing origins of hydrocarbons (Dai et al., 2005, 2009; Wu et al., 2017). However, the above isotopic signatures may not be sufficient to identify sources of hydrocarbons with multiple, similar source rocks. In addition to compound-specific isotope analysis, position-specific isotope analysis (PSIA) focuses on distributions of stable isotopes at different positions within a given molecule, and this potentially can provide valuable insights into the isotopic structures of hydrocarbons at the intramolecular scale. As the smallest organic molecule with non-equivalent carbon atoms (Galimov, 2006), various innovative approaches have been established to determine the position-specific (PS) isotope composition of propane (Gao et al., 2016; Gilbert et al., 2016; Liu et al., 2018a, 2023a; Piasecki et al., 2016, 2018), and PS isotopes have been applied to tracing the origins, investigating the generation process, and identifying the post-generation of hydrocarbons (Gilbert et al., 2019; Liu et al., 2019a, 2024, 2023b; Wang et al., 2024b).

In this study, we have established an improved approach for extracting adsorbed hydrocarbons from sediments based on thermal desorption technology and applied the technology to a tight sandstone gas reservoir from the Turpan-Hami Basin. We measured molecular and intramolecular carbon isotopic compositions of this gas reservoir and thermally desorbed hydrocarbons within potential sources to identify molecular- and intramolecular-scale relationship between the two types of gases. The results provided novel PS carbon isotope constraints on origins of hydrocarbons within the earth's crust.

2. Geological setting

The Turpan-Hami Basin, a Mesozoic-Cenozoic superimposed composite inland basin with about 5×10^4 km², is as one of the most important petroliferous basins in the Northwestern China (Fig. 1(a)) (Miao et al., 2023; Shao et al., 2003). The basin is bounded by the Bogda Mountain to the north, the Qoltag Mountain to the south, and the Harlik Mountain to the northeast. At present, it can be divided into three first-order tectonic units, including the Turpan Depression, the Liaodun Uplift and the Hami Depression from west to east (Fig. 1(b)). As a primary depression in the basin, the Turpan Depression consists of seven second-order tectonic units (Fig. 1(b)) (Gong et al., 2016; Shen et al., 2010).

Previous natural gas explorations in the Turpan-Hami Basin have confirmed that the discovered petroleum resources were mainly distributed in the Taibei Sag of the Turpan Depression (Gou et al., 2019). Recently, the resource potential of deep sandstone gases within the basin has been confirmed (Zhi et al., 2024). As natural gas exploration targets primary areas in the Turpan-Hami Basin (Ni et al., 2015), the Taibei Sag can be divided into three sub-sags, including the Shengbei Sub-sag, the Qiudong Sub-sag and the Xiaocaohu Sub-sag from west to east (Fig. 1(b)). In general, discovered petroleum in the basin mainly originates from the source rocks in the Permian Taodonggou Group and Jurassic Shuixigou Group (Gou et al., 2019). In addition, the geochemical characteristics of the tight sandstone gases in the Qiudong Sub-sag revealed that the hydrocarbons originate from humic organic matter in the Shuixigou Group (Liang et al., 2022). As one of the

important source rock strata of natural gases, the Jurassic Shuixigou Group includes the Middle Jurassic Xishanyao Fm. (J_2x) , the Lower Jurassic Sangonghe Fm. (J_1s) and the Lower Jurassic Badaowan Fm. (J_1b) (Fig. 2) (Su et al., 2009). Sediments within J_2x and J_1b are coalbearing deposits, and are considered as the main source rocks in the basin (Ni et al., 2015). However, sediments within J_1s generally consist of dark mudstone and silty mudstone at the upper section, and sandstone and pebbly sandstone at the lower section. Generally, no major coal seam is developed in J_1s .

3. Samples and methods

3.1. Samples

Mudstone samples were collected from different drilling wells in the Turpan-Hami Basin, including five mudstone samples and two coal samples from J_2x , seven source rock samples from J_1s , and two mudstone samples and one coal sample from J_1b . In addition, five deep tight sandstone gas samples were also collected from the Qiudong Sub-sag of the Turpan-Hami Basin.

3.2. Methods

3.2.1. Thermal desorption of hydrocarbons from source rock

In this study, hydrocarbons adsorbed onto the source rock samples are released and collected, using the improved thermal desorption apparatus (Fig. 3). In general, the apparatus includes a purge control system, a thermal desorption system and a detection system. The purge control system consists of high purity Ar (99.999%) and an AST10 gas mass flow controller (Asert Instrument (Beijing) Co., Ltd). The thermal desorption system mainly consists of a pyrolysis furnace (Hefei Kejing Materials Technology Co., Ltd), a quartz tube, two 2-way needle valves and a pressure meter (0–2 Mpa). The detection system includes a 6-way valve and a FULI 9790 Plus Gas Chromatograph (Zhejiang Fuli Analytical Instruments Corp.) equipped with a flame ionization detector (FID).

Firstly, the powder sample (20–40 mesh) was placed in the central part of the quartz tube in the pyrolysis furnace. Solid quartz rods were filled at both sides of the quartz tube to minimize the free volume. Then, the powder sample was purged by pure Ar for 10 min to remove the residual air in the quartz tube. Next, the two-way valves (A and B) were switched off and the powder sample was heated to 180 °C in 20min and kept for 120 min. As the gases desorbed from the surface of hydrocarbon source rock, the pressure within the thermal desorption system gradually increased. When the heating was completed, the two-way valve (B) was switched on, and the desorbed gas was introduced to the gas chromatograph for chemical analysis of the hydrocarbon gases via a six-port valve. During the experiment, the gas flow of Ar, the temperature of pyrolysis furnace and GC were controlled by the software. The GC oven with a capillary column (HP-PONA 50 m \times 0.20 mm i.d.) was initially set to 40 °C for 2 min, then was increased to 100 °C at 2 °C/ min, was finally increased to 260 °C at 20 °C/min and maintained at this temperature for 20 min. Only relative compositions of the desorbed gases (C₁-C₅) were determined to ensure that the concentrations of hydrocarbons were enough for CSIA and PSIA. The effluxes from the thermal desorption system were collected into an inverted container, which was filled and submerged in a NaCl saturated solution for both CSIA and PSIA.

3.2.2. Chemical composition

Chemical compositions of natural gas samples were determined by an Agilent 7890B gas chromatograph equipped with both flame ionization detector (FID) and thermal conductivity detector (TCD). Hydrocarbon gases (C_1 – C_5) were separated using a capillary

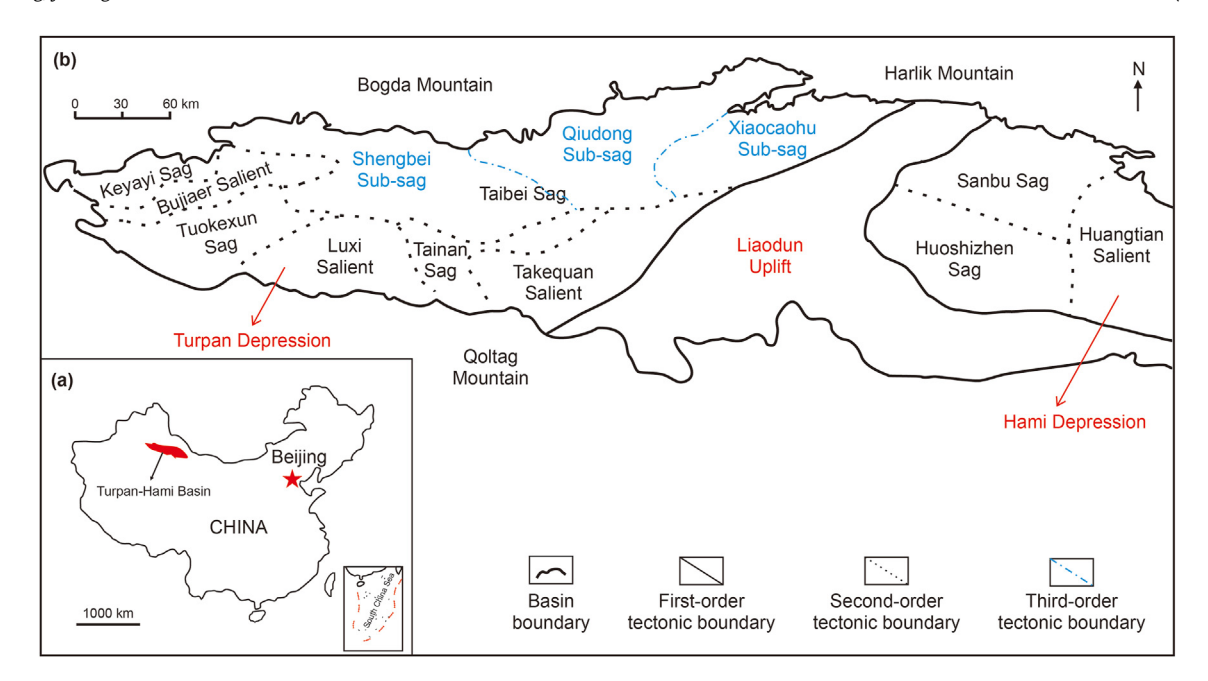


Fig. 1. (a) Location of the Turpan-Hami Basin. (b) The tectonic units of the Turpan-Hami Basin, modified from Gao et al. (2018) and Wang et al. (2024a).

column (HP-AL/S 25 m \times 0.32 mm i.d.). Inorganic gases were separated using a 5 Å molecular sieve packed column (2.44 m \times 3.15 mm i.d.). The GC oven was initially set to 60 °C, then was increased to 290 °C at 4 °C/min and maintained at this temperature for 15 min. Hydrocarbon gases (C_1 – C_5) and inorganic gases were detected in a single injection by precisely controlling the on-off states of the 6-way and 10-way valves.

3.2.3. Compound-specific carbon isotope composition

Compound-specific carbon isotope compositions of hydrocarbon gases (natural gases and thermally desorbed gases) were measured by a Thermo Scientific 253 Plus IRMS coupled to a Thermo Scientific Trace 1310 GC equipped with a capillary column (HP-PLOT Q 30 m \times 0.32 mm i.d.). The GC oven was initially set to 30 °C for 10 min, then was increased to 180 °C at 20 °C/min and maintained at this temperature for 2 min. The $\delta^{13}\text{C}$ values were reported relative to V-PDB in per mil (‰) with a precision within $\pm 0.5\%$.

3.2.4. PS carbon isotope composition

PS carbon isotope composition of propane was determined using the quantitative NMR calibrated GC-Py-GC-IRMS method described in our previous studies (Liu et al., 2023b, 2024; Wang et al., 2024b), and the measurement was conducted at the State Key Laboratory of Continental Dynamics, Department of Geology, Northwest University, China. The hydrocarbon gases were separated by the first GC column (HP-PLOT Q 30 m \times 0.32 mm i.d.). The temperature of the first GC oven was initially set at 50 °C for 3 min, further increased to 200 °C at 10 °C/min, and maintained at this temperature for 8 min. The separated compounds were then carried by high purity helium gas into a pyrolysis furnace ceramic reactor (50 cm, 0.7 mm i.d.) at 790 °C. The pyrolysis fragments of the gaseous hydrocarbons were separated by a second GC column (HP-PLOT Q 30 m \times 0.32 mm i.d.). The temperature of the second GC oven was initially set at 50 °C for 25 min, then increased to 200 °C at 20 °C/min, and maintained at this temperature for 5 min. The separated pyrolysis fragments were sequentially introduced into the combustion reactor of the GC-Isolink II and a Thermo Scientific 253 Plus IRMS to determine their carbon isotope values.

The GC columns and pyrolysis furnace were linked via a deactivated fused silica capillary column (0.25 mm i.d.). The calculation and calibration of $\Delta_{\text{C-T}}$, $\delta^{13}C_{\text{central}}$, and $\delta^{13}C_{\text{terminal}}$ values in propane were performed according to Gilbert et al. (2016) and Liu et al. (2023b).

4. Results

4.1. Chemical and compound-specific isotopic compositions of natural gases and thermal desorbed gases

Chemical compositions of the tight sandstone gases of the Qiudong Sub-sag show that the gas samples are dominated by hydrocarbon gases with an average proportion of 94.50% (Table 1). C_1 is a dominant gas and C_2 — C_5 concentrations decrease with increasing carbon number. Inorganic gases, N_2 and CO_2 , are in low proportions in most samples. However, the J701H sample contains a relatively high concentration of CO_2 (10.64%). The $\delta^{13}C$ values of hydrocarbons increase with increasing carbon number (Fig. 4(a)). The average $\delta^{13}C$ values of the C_1 , C_2 , C_3 , iC_4 , nC_4 , iC_5 and nC_5 are -41.0%, -27.8%, -27.0%, -25.8%, 25.8%, 25.8% and -24.6%, respectively.

In contract to the tight gas compositions, C_1-C_5 hydrocarbons in the thermally desorbed gases exhibit low concentrations, ranging from 0.45 to 14.68% with an average of 3.79%. C_3 is a primary gas of the thermally desorbed gases in the J_2x and J_1b source rocks, whereas C_1 serves as the principal component in a majority of the J_1s source rocks (Table 2). Apart from these components, no obvious difference in the other hydrocarbon gases of the thermally desorbed gases can be observed. For carbon isotopic distributions in alkane gases of the thermally desorbed gases, J10H, J702H-2, J10H-2 and J10H-3, generally shows a normal trend of increasing $\delta^{13}C$ values with increasing carbon number (Fig. 4(b)). However, several samples show reverse trends, i.e., $\delta^{13}C_1 > \delta^{13}C_2 > \delta^{13}C_3$ and $\delta^{13}C_2 > \delta^{13}C_3$. Majority samples exhibit a normal trend of carbon isotopes in C_3-C_5 (Fig. 4(b)).

 $\delta^{13}C_1$ values and the dryness have been used to distinguish thermogenic and microbial gases (Bernard et al., 1978; Whiticar, 1999). A Bernard diagram shows that the tight sandstone gases in

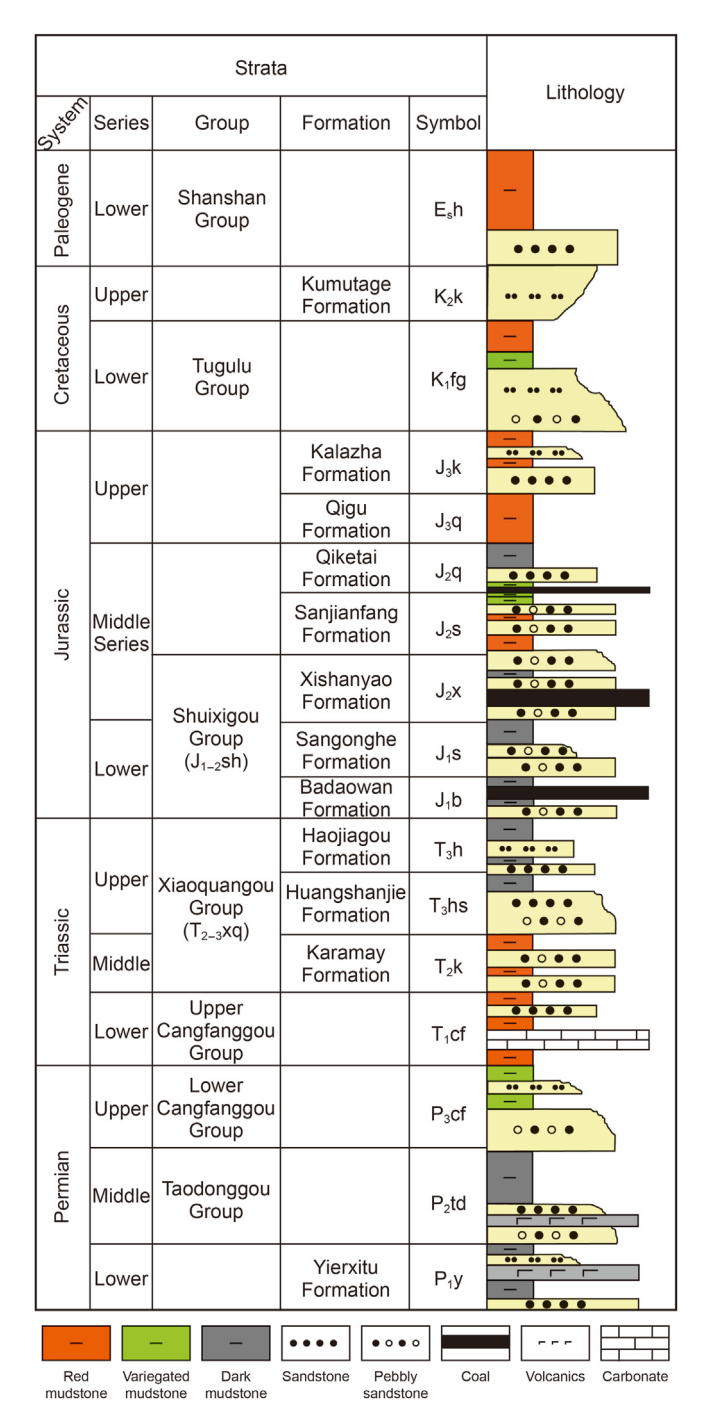


Fig. 2. Stratigraphic column of the Turpan-Hami Basin (modified from Gou et al. (2019) and Gong et al. (2016)).

this study are thermogenic gases (Fig. 5). In addition, different types of kerogens, humic organic matter (type III kerogen) and sapropelic organic matter (type I and II kerogen) generate light hydrocarbons with distinct $\delta^{13} C$ values (Buchardt et al., 1986; Whiticar, 1996), this relationship has been widely applied to identifying oil-type and coal-type thermogenic gases. All the tight sandstone samples in this study are thermogenic in origin and located near the coal-oil boundary (Fig. 6(a)). A $\delta^{13} C_2$ vs. $\delta^{13} C_1$ diagram shows that the natural gases in this study are similar to those from type III kerogen of the Niger delta and the Sacramento Basin (Fig. 6(b)), suggesting a humic origin.

4.2. PS carbon isotope of natural and thermal desorbed propane

The $\delta^{13}C_{central}$ values of propane in the tight gas samples range from -30.4% to -28.4% with an average of -29.1%, and the $\delta^{13}C_{terminal}$ values range from -26.5% to -25.2% with an average of -25.9%. The $\Delta_{C-T}(\delta^{13}C_{central}-\delta^{13}C_{termial})$ values of propane for the samples in this study show a narrow distribution from -3.9% to -2.4% with an average of -3.2%, indicating higher $\delta^{13}C$ values at the terminal positions compared to those at the central positions (Table 3).

PS carbon isotope compositions of the thermally desorbed propane from the source rocks in the different formations vary (Table 4). The average $\delta^{13}C_{central}$ values of propane from the source rocks in J_2x , J_1s and J_1b are -29.5, -29.0, and -25.6%, respectively, whereas the average $\delta^{13}C_{\text{terminal}}$ values are -24.3, -26.1, and -24.3%, respectively. The average Δ_{C-T} values of thermally desorbed propane of source rocks in J_2x , J_1s and J_1b are -5.2, -2.9, and -1.4%, respectively, indicating higher δ^{13} C values at the terminal positions compared to those at the central positions for the thermally desorbed propane from these potential source rocks. In addition, bulk and PS carbon isotopes of the thermally desorbed propane from the coal and mudstone of J₂x show similar distributions, suggesting similar isotopic structures of precursors in the coal and mudstone in J_2x . Compared with positive Δ_{C-T} values in coal-type gas reservoirs from the Ordos Basin, Sichuan Basin, and Bohai Bay Basin, the deep tight sandstone gases in this study and natural gases in the same basin (Liu et al., 2023b; Wang et al., 2024b) all have negative Δ_{C-T} values of propane (Fig. 7).

5. Discussion

5.1. Transport processes of natural and thermally desorbed hydrocarbons

After generation, hydrocarbons experience migration and accumulation processes before forming geological natural gas deposits, including diffusion and adsorption/desorption. Adsorption/ desorption on mineral surfaces and pores is an important postgeneration process, and isotopic fractionations of hydrocarbons during this process have been quantified (Wang et al., 2022; Xia and Tang, 2012). In a confined system with high proportion of adsorbed hydrocarbon gases, obvious carbon isotopic fractionation between free and adsorbed states can be observed, thereby causing to isotopic fractionation during desorption, and the larger isotope fractionations can be observed in methane during desorption compared to those in ethane (Liu et al., 2020). In addition, canister desorption experiments on freshly drilled shale core samples from the Ordos Basin have shown that the $\delta^{13}C_1$ and $\delta^{13}C_2$ values of desorbed gases increase with increasing extent of desorption. whereas the $\delta^{13}C_3$ values in desorbed gases remain almost constant (Meng et al., 2016). This suggests that significantly carbon isotopic fractionation cannot be observed during adsorption/desorption processes of propane in geological systems. Carbon isotope fractionation of diffusion is measured only for methane, but not for C₂+ hydrocarbon gases (Li et al., 2003; Schloemer and Krooss, 2004). The desorbed gases in this study represent the residual gases adsorbed on the pores and mineral surfaces, and these gases have different transport processes compared with gases in the reservoir rocks. Therefore, residual hydrocarbons in source rocks (adsorbed gases) and hydrocarbons in natural gas reservoirs may have different geochemical characteristics (e.g. chemical and isotopic compositions).

 $\delta^{13}C_1$ values of the thermally desorbed gases from the J₂x source rocks (JS1-1, J102–2 and J7-3) are obviously higher than tight sandstone gases and thermally desorbed gases from the J₁s source

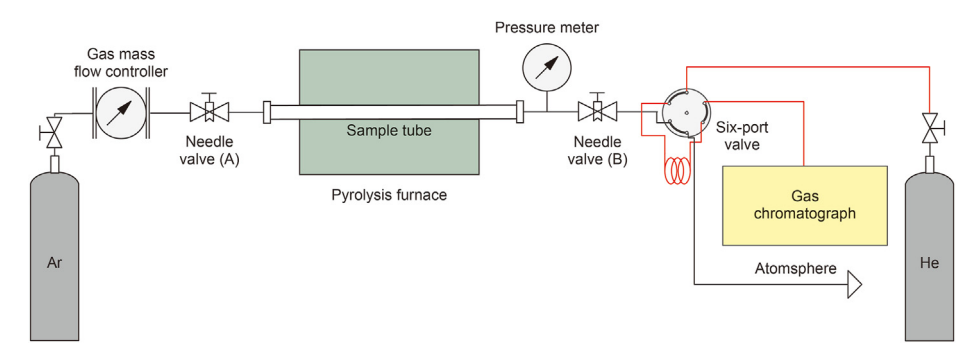


Fig. 3. Scheme of thermal desorption apparatus in this study.

 Table 1

 Chemical and carbon isotopic compositions of tight sandstone from the Qiudong Sub-sag, Turpan-Hami Basin.

Sample	Strata	Chemical composition, %								Compound-specific isotope composition, ‰							
		C_1	C ₂	C ₃	iC ₄	nC ₄	iC ₅	nC ₅	CO ₂	N ₂	C ₁	C ₂	C ₃	iC ₄	nC ₄	iC ₅	nC ₅
J701H	J ₂ x	68.52	9.87	5.72	1.41	1.57	0.52	0.44	10.64	1.26	-41.1	-26.9	-26.3	-25.4	-25.6	-25.7	-24.2
J703H-1	J_1s	70.31	12.45	8.06	1.93	2.17	0.64	0.54	2.18	1.72	-41.9	-28.3	-27.5	-26.0	-26.4	-25.8	-24.9
J7-2-3	J_1s	72.24	11.68	7.00	1.78	2.09	0.69	0.63	3.19	0.68	-40.0	-27.6	-26.9	-26.0	-25.4	-26.1	-24.7
J703H-2	J_2x	72.47	11.79	7.63	1.69	2.01	0.53	0.43	1.70	1.76	-41.9	-28.4	-27.8	-26.2	-26.8	-26.5	-24.9
J7H	J_1s	75.67	11.37	5.28	1.29	1.30	0.44	0.35	1.37	2.93	-40.3	-27.6	-26.4	-25.4	-24.8	-25.1	-24.2

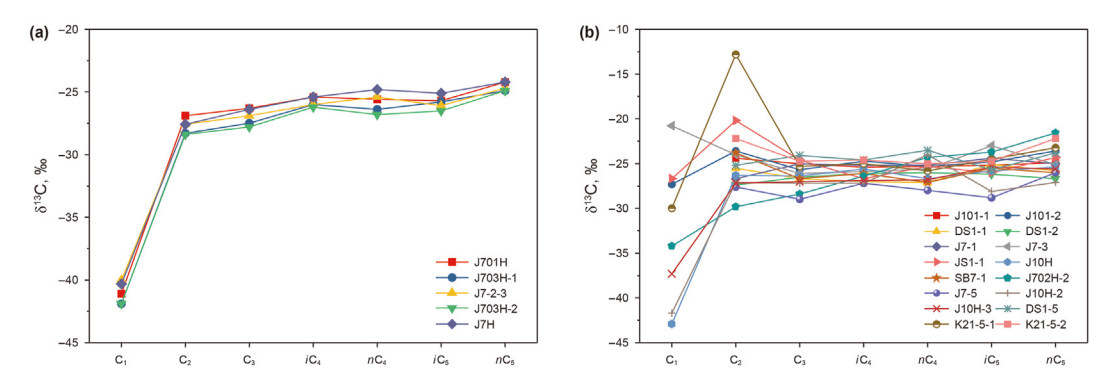


Fig. 4. $\delta^{13}C$ values of gaseous alkanes in (a) tight sandstone gases and (b) thermally desorbed gases.

Table 2Chemical and carbon isotopic compositions of thermally desorbed gases from the source rocks.

Sample	Lithology	Depth, m	Strata	Chemical composition, %					Compound-specific isotope composition, ‰								
				C ₁	C ₂	C ₃	iC ₄	nC ₄	iC ₅	nC ₅	C ₁	C_2	C ₃	iC ₄	nC ₄	iC ₅	nC ₅
J101-1	Mudstone	3841.92	J ₂ x	0.03	1.24	1.44	0.28	0.26	0.06	0.05	n.d.	-24.4	-25.0	-25.4	-25.3	-25.2	-24.9
J 101-2	Coal	3877.91	J_2x	0.06	1.53	2.67	0.96	0.73	0.18	0.13	-27.3	-23.6	-25.7	-24.7	-25.3	-24.8	-23.6
DS1-1	Mudstone	3683.15	J_2x	0.01	0.06	0.40	0.43	0.18	0.20	0.06	n.d.	-25.5	-26.7	-27.0	-27.1	-25.1	-25.8
DS1-2	Mudstone	3871.70	J_2x	0.03	0.45	0.53	0.18	0.13	0.06	0.04	n.d.	-27.4	-26.5	-26.1	-26.0	-26.2	-26.7
J7-1	Mudstone	4700.59	J_2x	0.03	0.83	0.71	0.09	0.21	0.04	0.06	n.d.	-26.7	-25.0	-25.2	-25.2	-24.4	-25.0
J7-3	Coal	5110.05	J_2x	0.02	1.29	3.60	0.22	0.37	0.06	0.10	-20.8	-24.0	-26.1	-25.9	-25.6	-23.0	-25.1
JS1-1	Mudstone	3572.92	J_2x	0.02	0.19	1.63	0.91	0.69	0.36	0.31	-26.7	-20.2	-24.6	-26.7	-25.3	-26.0	-24.3
J10H	Mudstone	5327.19	J_1s	1.88	0.73	0.46	0.12	0.16	0.07	0.06	-42.9	-26.3	-26.4	-25.6	-26.7	-25.8	-25.4
SB7-1	Mudstone	4558.10	J_1s	0.03	0.12	0.29	0.03	0.09	0.02	0.03	n.d.	-23.8	-26.7	-26.1	-27.1	-25.5	-26.0
J702H-2	Mudstone	5313.40	J_1s	10.51	3.03	0.73	0.11	0.18	0.07	0.06	-34.2	-29.8	-28.4	-26.4	-24.3	-23.7	-21.6
J7-5	Mudstone	5315.50	J_1s	0.03	0.88	0.71	0.09	0.21	0.04	0.06	n.d.	-27.6	-29.0	-27.2	-28.0	-28.8	-26.0
J10H-2	Mudstone	5328.99	J ₁ s	3.33	1.03	0.55	0.11	0.17	0.07	0.06	-41.7	-27.1	-27.2	-27.2	-24.0	-28.1	-27.1
J10H-3	Mudstone	5330.80	J ₁ s	3.38	1.30	0.77	0.18	0.28	0.10	0.10	-37.3	-27.2	-27.0	-26.9	-26.8	-25.4	-25.6
DS1-5	Mudstone	4300.88	J_1b	0.01	0.25	0.28	0.10	0.10	0.04	0.04	n.d.	-25.2	-24.1	-24.6	-23.5	-25.7	-23.8
K21-5-1	Coal	3464.58	J_1b	0.05	0.15	1.77	0.32	0.50	0.11	0.16	-30.0	-12.8	-25.3	-25.0	-25.8	-24.5	-23.2
K21-5-2	Mudstone	3459.00	J ₁ b	0.01	0.05	0.18	0.07	0.08	0.03	0.03	n.d.	-22.2	-24.7	-24.6	-25.0	-24.7	-22.2

rocks (J10H, J702H-2, J10H-2 and J10H-3) (Fig. 8(a)). Based on the $\delta^{13}C_1\text{--}R_0$ relationship of coal-type gas established by Chen et al.

(2021), the equivalent R_0 of the J_2x thermally desorbed gases exceed 2.5%, which are obviously inconsistent with the measured

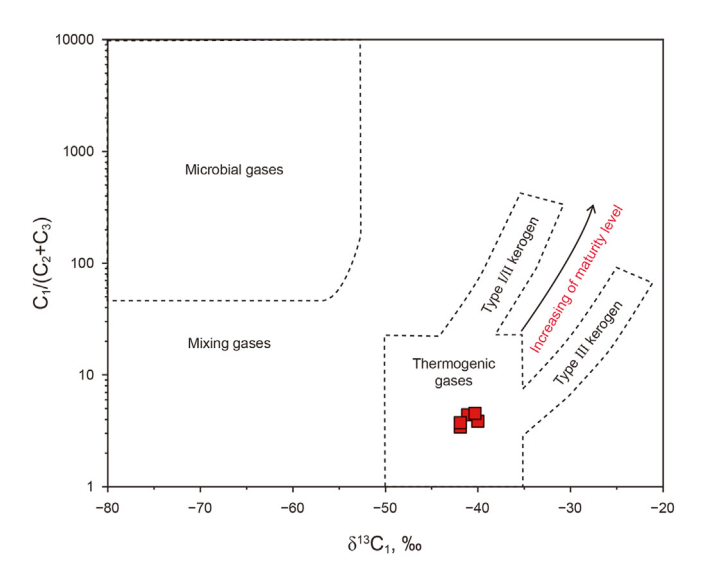


Fig. 5. Diagram of $C_1/(C_2+C_3)$ and $\delta^{13}C_1$ of the tight sandstone gas in the Qiudong Subsag, Turpan-Hami Basin. The identification polygons are modified from Bernard et al. (1978) and Whiticar (1999).

 R_0 of the J_2x source rocks (average: 0.8%). While, the $\delta^{13}C_1$ values of the tight sandstone gases fall within the $\delta^{13}C_1$ values of the J₁s thermally desorbed gases with a principal component of C₁. Therefore, chemical and isotopic fractionations likely occurred in residual C₁ during various post-generation processes. In addition, $\delta^{13}C_2$ values of the natural gas and thermally desorbed gas samples overlap well (Fig. 8(b)), while $\delta^{13}C_3$ values of the thermally desorbed gases from the J₂x and J₁s source rocks overlap slightly. However, a majority of the tight sandstone gases locate almost within the overlapped area of those two sets of the source rocks and the origins of hydrocarbons cannot be well interpreted by bulk δ¹³C₃ values alone. Carbon isotopic compositions of butane and pentane isomers of the natural and thermally desorbed gases exhibit similar distributions (Fig. 8(c) and (d)). These results suggest that the gaseous and isotopic compositions of C₁ (and possibly C2) from the thermally desorbed gases may had been altered by post-generation processes (Figs. 4 and 8(a)). Generally, the transport processes discussed above (diffusion and adsorption/desorption) induce increasingly smaller isotope fractionation, if any, with the increasing carbon number and δ^{13} C values of propane remain nearly constant during desorption process (Liu et al., 2020; Meng

Table 3PS carbon isotope composition of propane of tight sandstone from the Qiudong Subsag, Turpan-Hami Basin.

Sample	Strata	Position-s ‰	Position-specific carbon isotope composition, ‰						
		Δ_{C-T}	$\delta^{13}C_{central}$	$\delta^{13}C_{terminal}$					
J701H	J ₂ x	-3.2	-28.4	-25.2					
J703H-1	J_1s	-3.4	-29.8	-26.4					
J7-2-3	J_1s	-3.1	-28.9	-25.8					
J703H-2	J_2x	-3.9	-30.4	-26.5					
J7H	J_1s	-2.4	-28.1	-25.6					

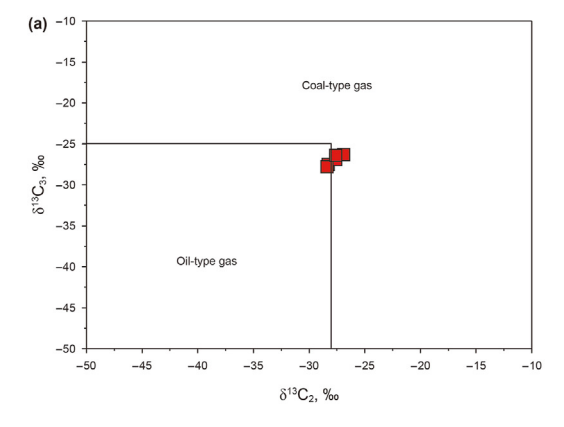
Table 4Bulk and PS isotones of propage in thermally desorbed hydrocarbons.

Sample	Lithology	Depth, m	Strata	Position-specific isotope composition, ‰					
				Δ_{C-T}	$\delta^{13}C_{central}$	$\delta^{13}C_{terminal}$			
J101-1	Mudstone	3841.92	J ₂ x	-3.2	-27.1	-23.9			
J101-2	Coal	3877.91	J_2x	-3.5	-28.0	-24.6			
DS1-1	Mudstone	3683.15	J ₂ x	-7.3	-31.6	-24.3			
DS1-2	Mudstone	3871.70	J_2x	-9.2	-32.7	-23.4			
J7-1	Mudstone	4700.59	J_2x	-7.1	-29.7	-22.6			
J7-3	Coal	5110.05	J_2x	-4.2	-28.9	-24.7			
JS1-1	Mudstone	3572.92	J_2x	-4.5	-27.6	-23.1			
J10H	Mudstone	5327.19	J_1s	-1.6	-27.4	-25.8			
SB7-1	Mudstone	4558.10	J_1s	-2.0	-28.0	-26.1			
J702H-2	Mudstone	5313.40	J_1s	-1.1	-29.2	-28.1			
J7-5	Mudstone	5315.50	J ₁ s	-2.3	-30.5	-28.2			
J10H-2	Mudstone	5328.99	J_1s	-2.9	-29.1	-26.2			
J10H-3	Mudstone	5330.80	J_1s	-3.1	-29.0	-25.9			
DS1-5	Mudstone	4300.88	J_1b	-3.2	-26.3	-23.1			
K21-5-1	Coal	3464.58	J_1b	-1.2	-26.1	-24.9			
K21-5-2	Mudstone	3459.00	J ₁ b	0.3	-24.5	-24.8			

et al., 2016; Wang et al., 2015a). Hence, C_3+ may have a better potential to correlate the natural gases and source rocks.

5.2. Precursor materials and propane generation revealed by PS isotope compositions $\,$

Compared with positive Δ_{C-T} values in coal-type gas reservoirs from the Ordos, Sichuan and Bohai Bay Basins (Fig. 7), the deep tight sandstone gases in this study and natural gases in the same basin from Liu et al. (2023b) and Wang et al. (2024b) all have negative Δ_{C-T} values of propane. Previously, two reaction pathways of thermogenic propane have been confirmed, n-propyl and i-



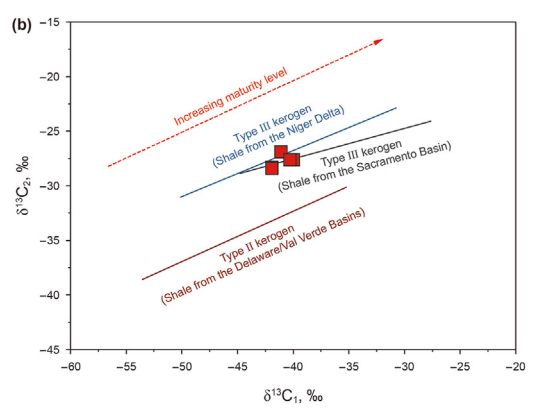


Fig. 6. (a) $\delta^{13}C_3$ vs. $\delta^{13}C_2$ for natural gases with different genetic types. The identification map is from Liu et al. (2019b). (b) $\delta^{13}C_2$ vs. $\delta^{13}C_1$ of tight sandstone gas in the Qiudong Subsag, Turpan-Hami Basin. The $\delta^{13}C_2$ and $\delta^{13}C_1$ values for gases from the type III kerogen of Niger Delta and the Type II kerogen from the Delaware/Val Verde Basin were reported by Rooney et al. (1995). The $\delta^{13}C_2$ and $\delta^{13}C_1$ values for gases from the Type III kerogen from the Sacramento Basin were reported by Jenden and Kaplan (1989).

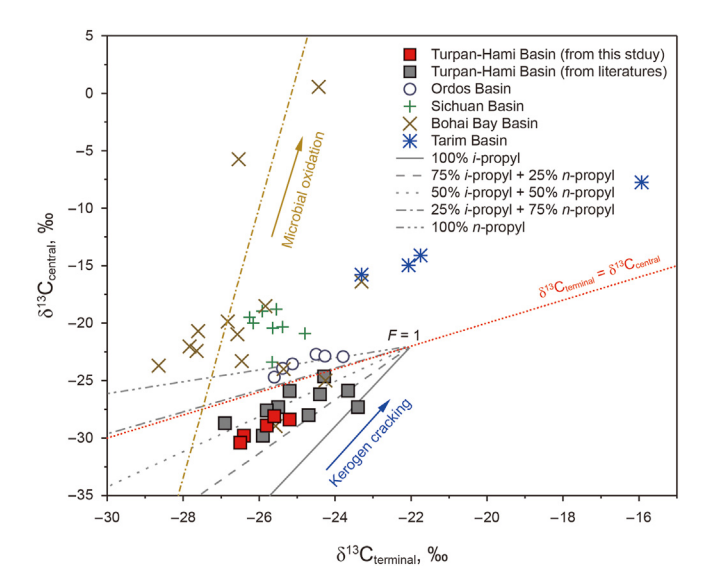


Fig. 7. $\delta^{13}C_{central}$ vs. $\delta^{13}C_{terminal}$ of propane in natural gases from different sedimentary basins. The PS carbon isotope composition of propane from thermal cracking of kerogen with different reaction pathways are from Wang et al. (2024b). The PS carbon isotope composition of propane from the Turpan-Hami Basin, Ordos Basin, Sichuan Basin, Bohai Bay Basin and Tarim Basin are from Liu et al. (2023b), Wang et al. (2024b) and this study. The linear trend illustrating the PS carbon isotope composition of propane for microbial oxidation is after Gilbert et al. (2019).

propyl reaction pathways (Liu et al., 2023b). The primary kinetic isotope effect (KIE) occurs on the central carbon position in the i-propyl reaction pathway, while it does on the terminal carbon position in the n-propyl reaction pathway. Therefore, the i-propyl reaction pathway produces propane of negative Δ_{C-T} values and the

n-propyl reaction pathway generates propane with positive $\Delta_{\text{C-T}}$ values. In early maturation stages, propane is generated mainly through the i-propyl radical pathway due to their lower activation energy than that of the n-propyl group (Hao et al., 2013; Liu et al., 2023b). As maturation increases and i-propyl group is consumed, propane generation pathway shifts to the n-propyl pathway. Thus, thermogenic propane at early maturations always has negative $\Delta_{\text{C-T}}$ values and $\Delta_{\text{C-T}}$ values of propane become positive with increasing thermal maturity levels of kerogen (Liu et al., 2023b, 2024; Wang et al., 2024b). The propane in the tight sandstone gases in this study appears to have mainly been generated from the i-propyl reaction pathways at an early maturation stage, but the n-propyl radical reaction also contributes to the propane generation in this study. No obvious microbial oxidation can be observed in the tight sandstone gas samples for this study (Fig. 7).

Fig. 9 shows that more n-propyl radical reaction involved in propane generation of the J₁s source rocks and that propane generated from the J₂x and j₁b source rocks mostly originates from the i-propyl radical reaction process, suggesting the higher proportion of branched chains in the J₂x and J₁b source rocks among the same types of precursors according to the kerogen chemical structure identification model proposed by Liu et al. (2024). For the thermally desorbed gases from I_1 s, more n-propyl radical reaction is involved in propane generation, leading to lower $\delta^{13}C_{terminal}$ values of propane compared with the propane from the J_2x and J_1b source rocks almost exclusively from the *i*-propyl radical reaction process. While, the thermally desorbed propane from J₁b source rock (K21-5-2) has positive Δ_{C-T} values, and other samples (DS1-5 and K21-5-1) have negative Δ_{C-T} values with different contributions of the *i*propyl and n-propyl radical reaction processes. Varying intramolecular carbon isotopic distributions within propane precursor kerogens provide us with a means to distinguish different chemical structures of parental kerogen types and maturity levels.

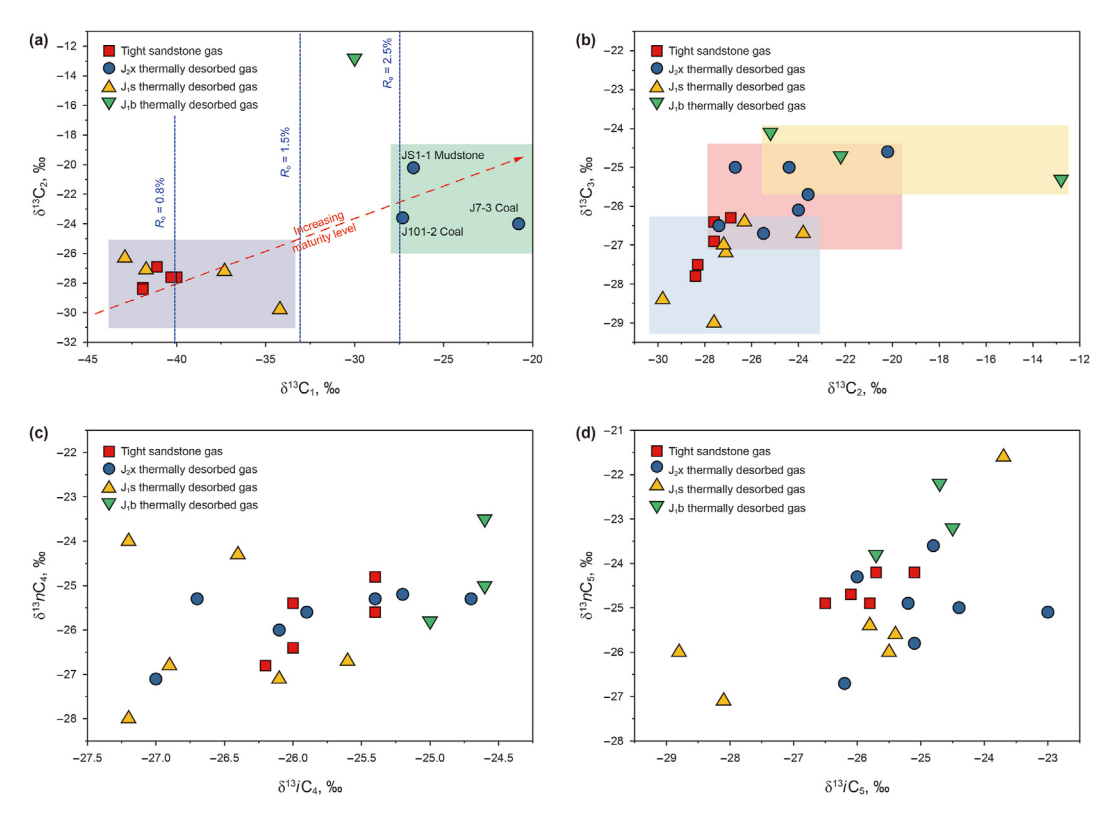


Fig. 8. (a) $\delta^{13}C_2$ vs. $\delta^{13}C_1$, (b) $\delta^{13}C_2$ vs. $\delta^{13}C_1$, (c) $\delta^{13}iC_2$ vs. $\delta^{13}nC_4$, and (d) $\delta^{13}iC_5$ vs. $\delta^{13}nC_5$ for tight sandstone gases and thermally desorbed gases from potential source rocks. The equivalent R_0 in Fig. 8(a) is from $\delta^{13}C_1$ - R_0 relationship of coal-type gas in Chen et al. (2021).

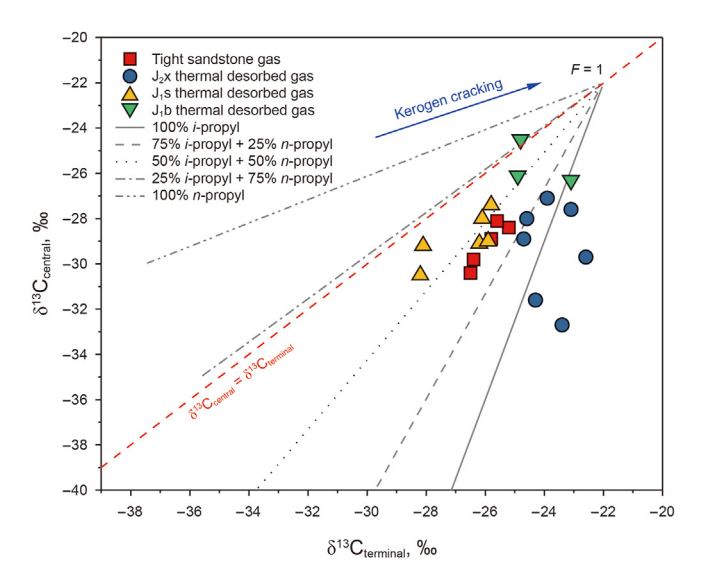


Fig. 9. $\delta^{13}C_{central}$ vs. $\delta^{13}C_{terminal}$ of propane in tight sandstone gases and thermally desorbed gases. The PS carbon isotope composition of propane from thermal cracking of kerogen with different reaction pathways are from Wang et al. (2024b).

5.3. Deciphering origins of hydrocarbons by intramolecular isotopic distributions

Other post-generation processes, such as microbial degradation and thermochemical sulfate reduction, could alter the initial chemical and isotopic compositions of propane. The $\delta^{13}C$ values of residual propane increase with increasing extent of microbial oxidation (Meng et al., 2017). Recent studies showed that microbial oxidation selectively oxidizes the central carbon and that $\delta^{13}C$ values at the central carbon position increase significantly, but those at the terminal carbon only slightly (Gilbert et al., 2019, 2022; Jaekel et al., 2014; Wang et al., 2024b). In addition, thermochemical sulfate reduction, an important chemical alteration of hydrocarbon during post-generation, also preferentially attacks the central carbon of propane (Xia and Gao, 2024). Therefore, $\delta^{13}C$ value at the terminal carbon positions of propane remains nearly constant with

increasing extent of microbial degradation and thermochemical sulfate reduction. Overall, the $\delta^{13}C_{terminal}$ value in propane is hardly affected by post-generation processes and could well record the isotopic composition of initially generated propane. Thus, the $\delta^{13}C_{terminal}$ value of propane can act as a strong indicator to decipher origins of hydrocarbons (Fig. 10).

Fig. 11 shows the δ^{13} C values at the two carbon positions vs. bulk δ^{13} C values of propane. The results show that the thermally desorbed propane from the source rock of J_1b has the larger $\delta^{13}C_3$ values, caused by the slightly higher maturity level of the J_1b source rock in the Qiudong Sub-sag (average R_0 : 1.10%) compared to that of the J_2x (average R_0 : 0.75%) and J_1s source rock (average R_0 : 0.82%). Bulk $\delta^{13}C_3$ values of the thermally desorbed propane from the J_2x and J_1s source rocks overlap slightly (Fig. 10(a)). On the other hand, the $\delta^{13}C_{\text{central}}$ value of the thermally desorbed propane from the J_2x source rocks highly overlaps with those of the thermal desorbed propane from the J_1s and J_1b source rocks. Since the data of the tight sandstone gases in this study locate almost within the overlapped area of the J_1s and J_2x source rocks (Fig. 11(a)), the source rocks of the tight sandstone gases cannot be readily inferred.

The thermally desorbed propane of the J₂x source rocks has higher bulk $\delta^{13}C_3$ and $\delta^{13}C_{terminal}$ values, compared to those of the J_1s source rock (Fig. 11(b)), but their $\delta^{13}C_{central}$ values are almost same (Fig. 11(a)). Compared with the coal-type gases from other basins, the tight sandstone gases and thermally desorbed gases in this study exhibit similar $\bar{\delta}^{13}C_{central}$ values compared with tight sandstone gases from the Ordos Basin. Natural gases from the Bohai Bay and Sichuan Basins have much higher $\delta^{13}C_{central}$ values than those from this study due to the microbial oxidation (Fig. 12(a)). Fig. 12(b) presents the $\delta^{13}C_{\text{terminal}}$ vs. $\delta^{13}C_3$ of propane from different coal-type gases and thermally desorbed gases. The results clearly show that the thermally desorbed propane from the source rock in J_2x have higher $\delta^{13}C_{terminal}$ values compared to those of the thermal desorbed propane from the J₁s source rock, and propane in the coal-type gases from the Bohai Bay and the Sichuan Basins (Fig. 12(b)).

In this study, the J_2x , J_1s and J_1b source rocks have no significant difference in their kerogen types. Hence, at similar maturity levels of kerogen cracking, they should have similar bulk $\delta^{13}C_3$, Δ_{C-T} , $\delta^{13}C_{central}$, and $\delta^{13}C_{terminal}$ values. However, the thermally desorbed

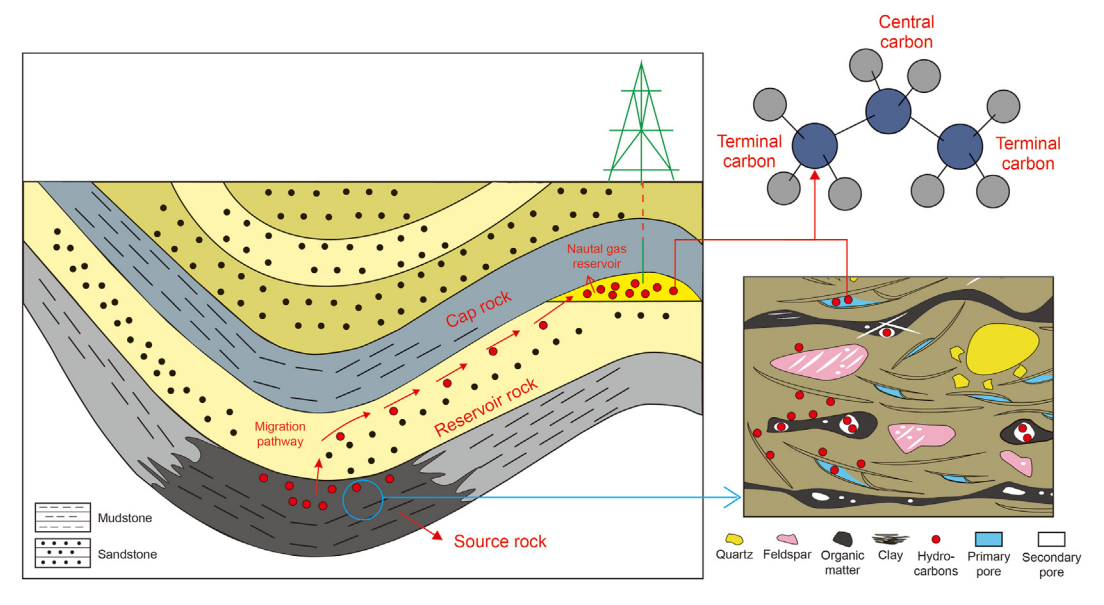


Fig. 10. Schematic for improved source-rock identification strategy. $\delta^{13}C_{\text{terminal}}$ value of propane in a reservoir is less susceptible to post generation processes, including migration, making it a useful gas-source correlation tool for hydrocarbon within the source rock.

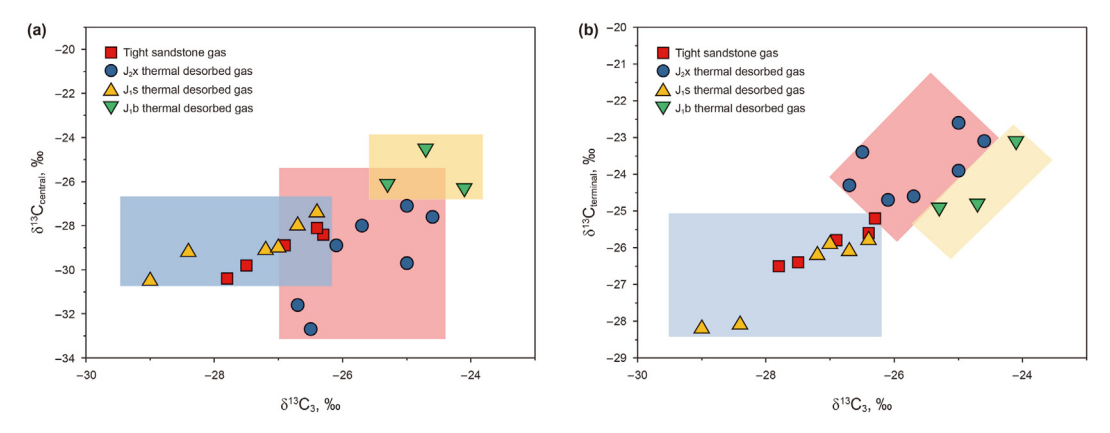


Fig. 11. $\delta^{13}C_{central}$ vs. $\delta^{13}C_3$ (a) and $\delta^{13}C_{terminal}$ vs. $\delta^{13}C_3$ (b) of propane from natural gas reservoirs and thermally desorbed gas of source rocks in the Qiudong Sub-sag, Turpan-Hami Basin.

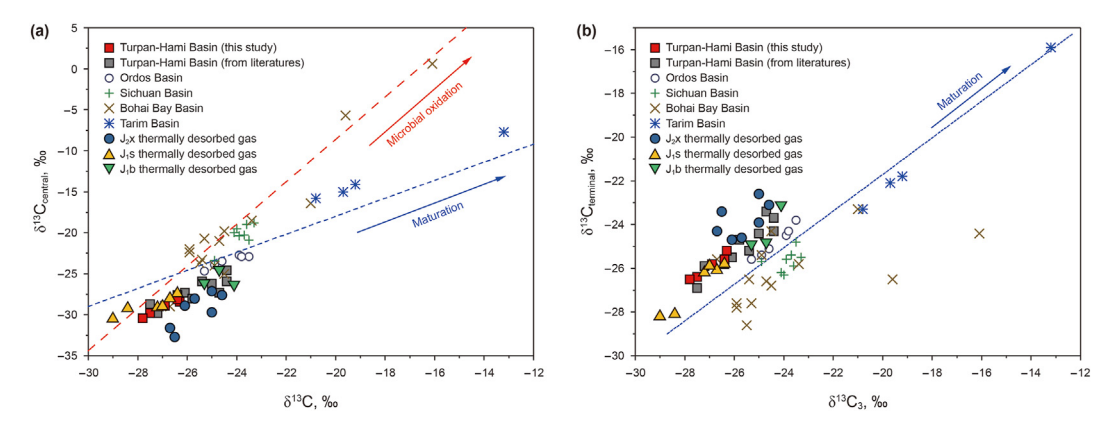


Fig. 12. δ^{13} C_{central} vs. δ^{13} C₃ (a) and δ^{13} C_{terminal} vs. δ^{13} C₃ (b) of propane from natural gas reservoirs from different basins and thermally desorbed propane of source rocks from the Turpan-Hami Basin. The bulk and PS isotope data of propane from the Turpan-Hami Basin, Ordos Basin, Sichuan Basin, Bohai Bay Basin and Tarim Basin are from Liu et al. (2023b), Wang et al. (2024b) and this study.

gases from the J_1s source rock have Δ_{C-T} values with an average of -2.2%, which are higher than these from the J_2x (-5.6%). Also, they have lower $\delta^{13}C_{terminal}$ values and similar $\delta^{13}C_{central}$ values. No obvious microbial oxidation can be observed in the tight sandstone gases for this study (Figs. 7 and 12(a)). Meanwhile, the thermally desorbed gases from the J_1s source rock exhibit lowest bulk $\delta^{13}C_3$ values among these potential source rocks. Hence, even though the source rocks from these different formations are humic organic matter (type III kerogen), minor differences exist in isotopic structures.

The $\delta^{13}C_{terminal}$ values of the thermal desorbed propane of the J_2x , J_1s and J_1b source rocks are largely separated (Fig. 11(b)), and data from the tight sandstone gas in this study fall within the $\delta^{13}C_{terminal}$ values of the thermal desorbed propane of the J_1s source rock. A genetic relationship indicated by the $\delta^{13}C_{terminal}$ values between the tight sandstone gas and the source rocks in J_1s strongly suggest that the tight sandstone gases in the Qiudong Sub-sag were generated from the J_1s source rocks.

6. Conclusions

Based on thermal desorption analysis of source rocks and intramolecular carbon isotopes analysis of propane, a direct identification method for the origins of hydrocarbons has been developed and applied first time to correlating gas-source relationship of the Jurassic deep tight sandstone gas in the Qiudong Sub-sag of the

Turpan-Hami Basin. The main conclusions are as follows:

- (1) Tight sandstone gases in this study originated from humic organic matter (type III kerogen) at early maturation stage.
- (2) The δ¹³C_{terminal} values of propane serves as a strong indicator in direct gas source correlation because the terminal carbons in propane are hardly affected by post-generation processes and could record the isotopic composition of initially generated propane.
- (3) Tight sandstone gases in the Qiudong Sub-sag are generated from the J_1 s mudstone based on the direct gas source correlation by intramolecular isotopes of thermally desorbed propane and natural propane.

CRediT authorship contribution statement

Peng Liu: Writing — original draft, Investigation, Funding acquisition, Data curation. **Xiao-Feng Wang:** Writing — review & editing, Supervision, Project administration, Methodology, Investigation. **Jie Wang:** Resources. **Juske Horita:** Writing — review & editing, Investigation, Funding acquisition. **Zhi-Yong Wang:** Resources, Investigation. **Ying Lin:** Writing — review & editing, Investigation. **Rui-Liang Guo:** Writing — review & editing. **Fu-Qi Li:** Investigation, Data curation. **Wen-Hui Liu:** Supervision, Investigation.

Declaration of competing interest

The authors declare that they have no known competing financial interests or personal relationships that could have appeared to influence the work reported in this paper.

Acknowledgment

This study was financially supported by the National Natural Science Foundation of China (Grant No. 42102202) and U. S. Department of Energy Geosciences program (DE-SC0016271). We would like to thank the reviewers for their valuable comments to improve the quality of the paper.

References

- Bernard, B.B., Brooks, J.M., Sackett, W.M., 1978. Light hydrocarbons in recent Texas continental shelf and slope sediments. J. Geophys. Res.: Oceans 83 (C8), 4053–4061. https://doi.org/10.1029/JC083iC08p04053.
- Buchardt, B., Clausen, J., Thomsen, E., 1986. Carbon isotope composition of lower palaeozoic kerogen: effects of maturation. Org. Geochem. 10 (1), 127–134. https://doi.org/10.1016/0146-6380(86)90016-1.
- Chen, J., Wang, X., Chen, J., et al., 2021. New equation to decipher the relationship between carbon isotopic composition of methane and maturity of gas source rocks. Sci. China Earth Sci. 64 (3), 470–493. https://doi.org/10.1007/s11430-020-9692-1
- Claypool, G.E., Threlkeld, C.N., Magoon, L.B., 1980. Biogenic and thermogenic origins of natural gas in Cook Inlet Basin, Alaska. AAPG Bull. 64 (8), 1131–1139. https://doi.org/10.1306/2F91944F-16CE-11D7-8645000102C1865D.
- Dai, J., Gong, D., Ni, Y., et al., 2014. Stable carbon isotopes of coal-derived gases sourced from the Mesozoic coal measures in China. Org. Geochem. 74, 123–142. https://doi.org/10.1016/j.orggeochem.2014.04.002.
- Dai, J., Li, J., Luo, X., et al., 2005. Stable carbon isotope compositions and source rock geochemistry of the giant gas accumulations in the Ordos Basin, China. Org. Geochem. 36 (12), 1617–1635. https://doi.org/10.1016/j.orggeochem.2005.08.017.
- Dai, J., Ni, Y., Zou, C., et al., 2009. Stable carbon isotopes of alkane gases from the Xujiahe coal measures and implication for gas-source correlation in the Sichuan Basin, SW China. Org. Geochem. 40 (5), 638–646. https://doi.org/10.1016/ j.orggeochem.2009.01.012.
- Etiope, G., Schoell, M., 2014. Abiotic gas: atypical, but not rare. Elements 10 (4), 291–296. https://doi.org/10.2113/gselements.10.4.291.
- Galimov, E.M., 1988. Sources and mechanisms of formation of gaseous hydrocarbons in sedimentary rocks. Chem. Geol. 71 (1), 77–95. https://doi.org/10.1016/0009-2541(88)90107-6.
- Galimov, E.M., 2006. Isotope organic geochemistry. Org. Geochem. 37 (10), 1200–1262. https://doi.org/10.1016/j.orggeochem.2006.04.009. Gao, G., Yang, S., Liang, H., et al., 2018. The origin and secondary alteration of dis-
- Gao, G., Yang, S., Liang, H., et al., 2018. The origin and secondary alteration of dissolved gas in oil: a case study from the western Tu-Ha Basin, China. J. Nat. Gas Sci. Eng. 52, 283–294. https://doi.org/10.1016/j.jngse.2018.01.044.
- Gao, L., He, P., Jin, Y., et al., 2016. Determination of position-specific carbon isotope ratios in propane from hydrocarbon gas mixtures. Chem. Geol. 435, 1–9. https:// doi.org/10.1016/j.chemgeo.2016.04.019.
- Gilbert, A., Nakagawa, M., Taguchi, K., et al., 2022. Hydrocarbon cycling in the tokamachi mud volcano (Japan): insights from isotopologue and metataxonomic analyses. Microorganisms 10 (7), 1417. https://doi.org/10.3390/microorganisms10071417.
- Gilbert, A., Sherwood, Lollar B., Musat, F., et al., 2019. Intramolecular isotopic evidence for bacterial oxidation of propane in subsurface natural gas reservoirs. Proc. Natl. Acad. Sci. USA 116 (14), 6653–6658. https://doi.org/10.1073/pnas.1817784116.
- Gilbert, A., Yamada, K., Suda, K., et al., 2016. Measurement of position-specific ¹³C isotopic composition of propane at the nanomole level. Geochem. Cosmochim. Acta 177, 205–216. https://doi.org/10.1016/j.gca.2016.01.017.
- Gong, D., Cao, Z., Ni, Y., et al., 2016. Origins of Jurassic oil reserves in the Turpan—Hami Basin, northwest China: evidence of admixture from source and thermal maturity. J. Petrol. Sci. Eng. 146, 788—802. https://doi.org/10.1016/j.petrol.2016.07.025.
- Gou, H.G., Zhang, P., She, J.C., et al., 2019. Petroleum geological conditions, resource potential and exploration direction in Turpan-Hami Basin. Marine Origin Petroleum Geology 24 (2), 85–96. https://doi.org/10.11764/j.issn.1672-1926.2018.08.021 (in Chinese).
- Hao, Y.L., Li, J.L., Wei, Z.H., et al., 2013. Molecular simulation on pyrolysis mechanism of butane. Acta Pet. Sin. 29 (5), 824–829. https://doi.org/10.3969/j.issn.1001-8719.2013.05.013 (in Chinese).
- Jaekel, U., Vogt, C., Fischer, A., et al., 2014. Carbon and hydrogen stable isotope fractionation associated with the anaerobic degradation of propane and butane by marine sulfate-reducing bacteria. Environ. Microbiol. 16 (1), 130–140. https://doi.org/10.1111/1462-2920.12251.
- Jenden, P., Kaplan, I., 1989. Origin of natural gas in Sacramento Basin, California.

AAPG Bull. 73 (4), 431–453. https://doi.org/10.1306/44B49FC9-170A-11D7-8645000102C1865D.

- Julien, M., Goldman, M.J., Liu, C., et al., 2020. Intramolecular ¹³C isotope distributions of butane from natural gases. Chem. Geol. 541, 119571. https://doi.org/10.1016/j.chemgeo.2020.119571.
- Li, J., Liu, Z., Li, Z., et al., 2003. Experiment investigation on the carbon isotope and composition fractionation of methane during gas migration by diffusion. Nat. Gas Geosci. 14 (6), 463–468. https://doi.org/10.3969/j.issn.1672-1926.2003.06.008 (in Chinese).
- Liang, S., Qian, F., Xiao, D., 2022. Exploration discovery and implications of the jurassic tight sandstone oil and gas reservoir in well Ji7H in Taibei sag, Turpan-Hami Basin. China Petrol Explorat. 27 (1), 50. https://doi.org/10.3969/ j.issn.1672-7703.2022.01.005 (in Chinese).
- Liu, C., Liu, P., McGovern, G.P., et al., 2019a. Molecular and intramolecular isotope geochemistry of natural gases from the Woodford Shale, Arkoma Basin, Oklahoma. Geochem. Cosmochim. Acta 255, 188–204. https://doi.org/10.1016/ j.gca.2019.04.020.
- Liu, C., Liu, P., Wang, X., et al., 2023a. Establishing accuracy of position-specific carbon isotope analysis of propane by GC-Pyrolysis-GC-IRMS. Rapid Commun. Mass Spectrom. e9494. https://doi.org/10.1002/rcm.9494.
- Liu, C., McGovern, G.P., Liu, P., et al., 2018a. Position-specific carbon and hydrogen isotopic compositions of propane from natural gases with quantitative NMR. Chem. Geol. 491, 14–26. https://doi.org/10.1016/j.chemgeo.2018.05.011.
- Liu, P., Wang, X., Lin, Y., et al., 2020. Chemical and carbon isotope fractionations of alkane gases desorbed from confined systems and the application toward shale gas reservoir. Mar. Petrol. Geol. 113, 104103. https://doi.org/10.1016/ j.marpetgeo.2019.104103.
- Liu, P., Wang, X., Liu, C., et al., 2024. Intramolecular carbon isotopic rollover in propane from natural gas reservoirs of the Santanghu Basin: insights into chemical structure of kerogen. Org. Geochem. 188, 104740. https://doi.org/10.1016/j.orggeochem.2024.104740.
- Liu, P., Wang, X., Liu, C., et al., 2023b. Kinetic isotope effects and reaction pathways of thermogenic propane generation at early maturation stage: insights from position-specific carbon isotope analysis. Mar. Petrol. Geol. 153, 106252. https://doi.org/10.1016/j.marpetgeo.2023.106252.
- Liu, Q., Chen, M., Liu, W., et al., 2009. Origin of natural gas from the Ordovician paleo-weathering crust and gas-filling model in Jingbian gas field, Ordos basin, China. J. Asian Earth Sci. 35 (1), 74–88. https://doi.org/10.1016/j.jseaes.2009.01.005.
- Liu, Q., Jin, Z., Li, H., et al., 2018b. Geochemistry characteristics and genetic types of natural gas in central part of the Tarim Basin, NW China. Mar. Petrol. Geol. 89, 91–105. https://doi.org/10.1016/j.marpetgeo.2017.05.002.
- Liu, Q., Jin, Z., Li, J., et al., 2012. Origin of marine sour natural gas and gas-filling model for the Wolonghe Gas Field, Sichuan Basin, China. J. Asian Earth Sci. 58, 24–37. https://doi.org/10.1016/j.jseaes.2012.07.007.
- Liu, Q., Jin, Z., Meng, Q., et al., 2015. Genetic types of natural gas and filling patterns in Daniudi gas field, Ordos Basin, China. J. Asian Earth Sci. 107, 1–11. https:// doi.org/10.1016/j.jseaes.2015.04.001.
- Liu, Q., Jin, Z., Wang, X., et al., 2018c. Distinguishing kerogen and oil cracked shale gas using H, C-isotopic fractionation of alkane gases. Mar. Petrol. Geol. 91, 350–362. https://doi.org/10.1016/j.marpetgeo.2018.01.006.
- Liu, Q., Wu, X., Wang, X., et al., 2019b. Carbon and hydrogen isotopes of methane, ethane, and propane: a review of genetic identification of natural gas. Earth Sci. Rev. 190, 247–272. https://doi.org/10.1016/j.earscirev.2018.11.017.
- Liu, W., Chen, M., Guan, P., et al., 2007. Ternary geochemical-tracing system in natural gas accumulation. Sci. China Earth Sci. 50 (10), 1494–1503. https://doi.org/10.1007/s11430-007-0091-z.
- Liu, W., Xu, Y., 1999. A two-stage model of carbon isotopic fractionation in coal-gas. Geochimica 28 (4), 359–366 (in Chinese). https://doi.org/10.19700/j.0379-1726. 1999.04.006.
- Meng, Q., Wang, X., Wang, X., et al., 2017. Gas geochemical evidences for biodegradation of shale gases in the upper triassic yanchang formation, Ordos Basin, China. Int. J. Coal Geol. 179, 139–152. https://doi.org/10.1016/j.coal.2017.05.018.
- Meng, Q., Wang, X., Wang, X., et al., 2016. Variation in the carbon isotopic composition of alkanes during shale gas desorption process and its geological significance. J Nat Gas Geosci. 1 (2), 139–146. https://doi.org/10.1016/ j.jnggs.2016.05.004.
- Miao, H., Guo, J., Wang, Y., et al., 2023. Mineralogical and elemental geochemical characteristics of Taodonggou group mudstone in the Taibei sag, turpan—hami basin: implication for its formation mechanism. Solid Earth 14 (9), 1031–1052. https://doi.org/10.5194/se-14-1031-2023.
- Ni, Y., Zhang, D., Liao, F., et al., 2015. Stable hydrogen and carbon isotopic ratios of coal-derived gases from the Turpan-Hami Basin, NW China. Int. J. Coal Geol. 152, 144–155. https://doi.org/10.1016/j.coal.2015.07.003.
- Piasecki, A., Sessions, A., Lawson, M., et al., 2016. Analysis of the site-specific carbon isotope composition of propane by gas source isotope ratio mass spectrometer. Geochem. Cosmochim. Acta 188, 58–72. https://doi.org/10.1016/i.gca.2016.04.048.
- Piasecki, A., Sessions, A., Lawson, M., et al., 2018. Position-specific ¹³C distributions within propane from experiments and natural gas samples. Geochem. Cosmochim. Acta 220, 110–124. https://doi.org/10.1016/j.gca.2017.09.042.
- Rooney, M.A., Claypool, G.E., Moses, Chung H., 1995. Modeling thermogenic gas generation using carbon isotope ratios of natural gas hydrocarbons. Chem. Geol. 126 (3), 219–232. https://doi.org/10.1016/0009-2541(95)00119-0.
- Schloemer, S., Krooss, B., 2004. Molecular transport of methane, ethane and

nitrogen and the influence of diffusion on the chemical and isotopic composition of natural gas accumulations. Geofluids 4 (1), 81–108. https://doi.org/10.1111/j.1468-8123.2004.00076.x.

- Schoell, M., 1980. The hydrogen and carbon isotopic composition of methane from natural gases of various origins. Geochem. Cosmochim. Acta 44 (5), 649–661. https://doi.org/10.1016/0016-7037(80)90155-6.
- Schoell, M., 1983. Genetic characterization of natural gases. AAPG Bull. 67 (12), 2225–2238. https://doi.org/10.1306/ad46094a-16f7-11d7-8645000102c1865d.
- Schoell, M., 1988. Multiple origins of methane in the Earth. Chem. Geol. 71 (1), 1–10. https://doi.org/10.1016/0009-2541(88)90101-5.
- Shao, L., Zhang, P., Hilton, J., et al., 2003. Paleoenvironments and paleogeography of the Lower and lower Middle Jurassic coal measures in the Turpan-Hami oilprone coal basin, northwestern China. AAPG Bull. 87 (2), 335–355. https:// doi.org/10.1306/09160200936.
- Shen, P., Wang, X., Wang, Z., et al., 2010. Geochemical characteristics of light hydrocarbons in natural gases from the Turpan-Hami Basin and identification of low-mature gas. Chin. Sci. Bull. 55 (29), 3324–3328. https://doi.org/10.1007/s11434-010-4011-9.
- Smith, J.W., Pallasser, R.J., 1996. Microbial origin of Australian coalbed methane. AAPG Bull. 80 (6), 891–897. https://doi.org/10.1306/64ED88FE-1724-11D7-8645000102C1865D.
- Stahl, W.J., Carey, B.D., 1975. Source-rock identification by isotope analyses of natural gases from fields in the Val Verde and Delaware basins, west Texas. Chem. Geol. 16 (4), 257–267. https://doi.org/10.1016/0009-2541(75)90065-0.
- Su, C.G., Huang, W.D., Bai, J.X., et al., 2009. Natural gas accumulation conditions and controlled factors in Turpan-Hami basin. Nat. Gas Geosci. 20 (1), 51–56. https://doi.org/10.11764/j.issn.1672-1926.2018.08.021 (in Chinese).
- Vandré, C., Cramer, B., Gerling, P., et al., 2007. Natural gas formation in the western Nile delta (Eastern Mediterranean): thermogenic versus microbial. Org. Geochem. 38 (4), 523–539. https://doi.org/10.1016/j.orggeochem.2006.12.006.
- Wang, B., Huang, Z., Xiao, D., et al., 2024a. Generation and expulsion of lower jurassic hydrocarbon in different source rocks in the Taibei sag, Turpan-Hami Basin, northwest China. J. Asian Earth Sci. 259, 105911. https://doi.org/ 10.1016/j.iseaes.2023.105911.
- Wang, X., Li, X., Wang, X., et al., 2015a. Carbon isotopic fractionation by desorption

- of shale gases. Mar. Petrol. Geol. 60, 79-86. https://doi.org/10.1016/j.marpetgeo.2014.11.003.
- Wang, X., Liu, P., Liu, W., et al., 2024b. Intramolecular carbon isotope of propane from coal-derived gas reservoirs of sedimentary basins: implications for source, generation and post-generation of hydrocarbons. Geosci. Front. 15 (4), 101806. https://doi.org/10.1016/j.gsf.2024.101806.
- Wang, X., Liu, P., Meng, Q., et al., 2022. Physical selectivity on isotopologues of gaseous alkanes by shale pore network: evidence from dynamic adsorption process of natural gas. J. Nat. Gas Sci. Eng. 97, 104252. https://doi.org/10.1016/i.ingse.2021.104252.
- Wang, X., Liu, W., Shi, B., et al., 2015b. Hydrogen isotope characteristics of thermogenic methane in Chinese sedimentary basins. Org. Geochem. 83, 178–189. https://doi.org/10.1016/j.orggeochem.2015.03.010.
- Whiticar, M.J., 1996. Stable isotope geochemistry of coals, humic kerogens and related natural gases. Int. J. Coal Geol. 32 (1), 191–215. https://doi.org/10.1016/S0166-5162(96)00042-0.
- Whiticar, M.J., 1999. Carbon and hydrogen isotope systematics of bacterial formation and oxidation of methane. Chem. Geol. 161 (1), 291–314. https://doi.org/10.1016/S0009-2541(99)00092-3.
- Wu, X., Liu, Q., Zhu, J., et al., 2017. Geochemical characteristics of tight gas and gassource correlation in the Daniudi gas field, the Ordos Basin, China. Mar. Petrol. Geol. 79, 412–425. https://doi.org/10.1016/j.marpetgeo.2016.10.022.
- Xia, X., Gao, Y., 2024. Compound-specific, intra-molecular, and clumped 13C fractionations in the thermal generation and decomposition of ethane and propane: a DFT and kinetic investigation. Geochem. Cosmochim. Acta 375, 50–63. https://doi.org/10.1016/j.gca.2024.05.001.
- Xia, X., Tang, Y., 2012. Isotope fractionation of methane during natural gas flow with coupled diffusion and adsorption/desorption. Geochem. Cosmochim. Acta 77, 489–503. https://doi.org/10.1016/j.gca.2011.10.014.
- Xu, Y., 1994. Origin Theory and Application of Natural Gas. Science Press, Beijing, pp. 1–414 (in Chinese).
- Zhi, D., Li, J., Yang, F., et al., 2024. Exploration breakthrough and significance of Jurassic tight sandstone gas in Qiudong subsag of Tuha Basin. Acta Pet. Sin. 45 (2), 348–357. https://doi.org/10.7623/syxb202402002 (in Chinese).